Available online at www.sciencedirect.com
ScienceDirect
European Journal of Mechanics B/Fluids 26 (2007) 295–303

# High velocity flow through fractured and porous media: the role of flow non-periodicity

Yann Lucas *, Mikhail Panfilov, Michel Buès

*Laboratoire, Environnement, Géomécanique et Ouvrages, ENSG-INPL, rue du doyen Roubault, 54501 Vandoeuvre-lès-Nancy cedex, France*

Received 27 September 2005; received in revised form 22 March 2006; accepted 22 April 2006

Available online 13 July 2006

**Abstract**

In the present paper we examine the evolution of the macroscopic flow law in a crenellated channel, representing an element of fractured or porous medium and in function of the Reynolds number *Re*. A numerical analysis based on the Navier–Stokes equations is applied. We focus on the influence of the flow periodicity or non-periodicity upon the macroscopic law. The physical explanation of the non-linear deviation from Darcy's law is still an issue, as the Ergun–Forchheimer law admitted for high Reynolds numbers comes up against some theoretical problems. In the periodic case, three non-linear flow regimes were revealed: a cubic flow with respect to velocity at low *Re*, an intermediate non-quadratic law, and a self-similar mode independent of *Re* at very high *Re*. The Forchheimer law is not confirmed. The case of a non-periodic flow clearly highlights the link between the flow non-periodicity and the quadratic law. The quadratic deviation becomes all the more important as the non-periodicity degree is high.


*Keywords:* Cubic deviation; Quadratic law; Forchheimer; Inertia; Laminar flow; Periodicity; Fracture; Porous media

## 1. Introduction: concerning the non-linear deviations from Darcy's law

Darcy's law adequately describes flow in porous media at low velocity. At high velocity, a situation observed near gas–oil–water wells, the valid flow law is an open problem. This question has however a major economic impact, being in the bases of the well test interpretation and data acquisition.

Many experiments and numerical studies show that Darcy's law should be corrected by a cubic term in velocity, starting from a certain value of the Reynolds number. The latter will be transformed into a quadratic one, which goes under the name of Forchheimer's law (e.g., [1]), when the Reynolds number increases. The cubic flow, sometimes called the weak inertia regime (e.g., [1,2]), is understood as that regime at which the inertial force is of the same order as the viscous force. In quadratic flow, the inertial force is predominant, so it is called the strong inertia regime. At the same time, the physical understanding of the generally accepted quadratic law is not obvious.

Despite of some attempts to theoretically prove the quadratic law [3,4], the detailed mathematical analysis of flow and the influence of the equation non-linearities on the flow structure revealed some paradoxes [5,6]. In particular, it was shown that the quadratic term is not in agreement with the symmetry conditions, which require that the pressure

* Corresponding author. Tel.: +33 383 596319; fax: +33 383 596300.
*E-mail address:* yann.lucas@ensg.inpl-nancy.fr (Y. Lucas).

0997-7546/$ – see front matter 
doi:10.1016/j.euromechflu.2006.04.005

gradient expansion over velocity contains only the odd terms in an isotropic medium [7]. So the quadratic term should disappear.

In the same type of idea, a cubic deviation from Darcy's law, not however quadratic, was obtained by homogenisation of the Navier–Stokes equations in isotropic case [8–10].

Another explanation to the quadratic law is turbulence. It was shown in [2] that the turbulent flow leads to a Forchheimer-type macroscopic law. Nevertheless, it was shown experimentally and numerically that the quadratic deviation appears within the laminar flow regime [11]. It is for this reason that the turbulent case is not examined in the present paper.

Within the framework of laminar flow, the resolution of paradoxes induced by the quadratic law can be obtained only if the flow becomes microscopically asymmetric, or irregular, as shown in [6]. In this paper we only examine the influence of the flow asymmetry (non-periodicity). Our analysis will be focused on a stable and stationary flow which is observed experimentally until the Reynolds number reaches a critical value [12] in the order of 2000.

We analyse the model of a crenellated channel, as in previous works [13,14]. This is a classic model of porous or fractured medium which ensures non-zero inertia effects and takes into account the staggers of solid material, in contrast to a uniform channel where no staggers and no inertia are observed. The analysis is based on numerical simulation. This enables us to study the macroscopic flow law and its evolution with the Reynolds number, depending on the flow structure inside channel.

This paper is organised as follows. In Section 2, we formulate the problem of flow in a channel and in the overall porous medium, by introducing a channel cell and a general form of the non-linear macroscopic flow equation. In Section 3, we study the periodic flow, the problem of how to produce it numerically, and we discuss the resulting various deviations from Darcy's law. In Sections 4 and 5, we study a non-periodic flow and its influence on the non-linear deviation. Conclusions are summarised in Section 6.

## 2. Problem formulation

### 2.1. Microscopic flow in a non-uniform channel

The following two-dimensional cell of a fractured or porous medium is considered (Fig. 1):

The incompressible flow governed by the steady-state Navier–Stokes equations with respect to velocity $\boldsymbol{v}$ and pressure $p$ is considered in the domain $Y_\mathrm{f}$ of a cell $Y = Y_\mathrm{f} \cup Y_\mathrm{s}$, where $Y_\mathrm{f}$ is occupied with the fluid and $Y_\mathrm{s}$ is the solid:

$$\rho v_i \frac{\partial v_j}{\partial x_i} = -\frac{\partial p}{\partial x_j} + f_j + \mu \Delta v_j, \quad \frac{\partial v_i}{\partial x_i} = 0, \quad \forall M \in Y_\mathrm{f}, \quad i, j = 1, 2, \tag{1}$$

where $\rho$ and $\mu$ are the density and the dynamic viscosity, $f$ is the volumetric force. The fluid velocity is zero at the walls:

$$v_i = 0, \quad \forall M \in \partial Y_\mathrm{fs}, \quad i = 1, 2. \tag{2}$$

The boundary-value conditions which are imposed at the cell inlet and outlet depend on the examined problem. The bottom boundary is a symmetry axis. The fluid enters through AA′ and leaves the cell through BB′.

Such a problem will be called "microscopic", while the term "macroscopic" will be attributed to a flow averaged over the cell.

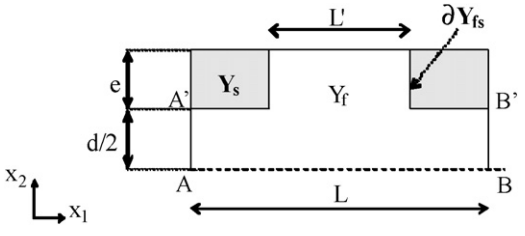


Fig. 1. Cell Y of porous medium.

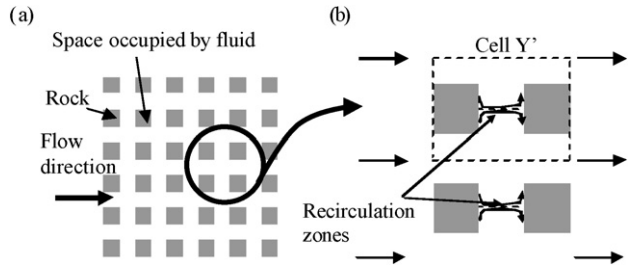


Fig. 2. Flow around solid particles as another model of porous media (a) and the analogy of a cell with the crenellated channel (b).

The configuration of a crenellated channel is able to describe the flow in other types of porous media. For instance, the periodic lattice of obstacles shown in Fig. 2(a) has a unite cell $Y'$ (Fig. 2(b)) which is almost equal to the geometry in Fig. 1.

### 2.2. Macroscopic flow law

As the macroscopic flow is directed along $x_1$, we can define macroscopic pressure $P$ and velocity $\boldsymbol{V}$ as follows:

$$P(x_1) = \frac{1}{|S(x_1)|} \int\limits_{S(x_1)} p(x_1, x_2)\,\mathrm{d}x_2, \qquad \boldsymbol{V}(x_1) = \frac{1}{|S(x_1)|}\left( \int\limits_{S(x_1)} \boldsymbol{v}(x_1, x_2) \cdot \boldsymbol{e}_1\,\mathrm{d}x_2 \right)\boldsymbol{e}_1, \tag{3}$$

where $S(x_1)$ is the vertical cross-section, $|S(x_1)|$ is the cross-section area and $\boldsymbol{e}_1$ is the unit vector along $x_1$. As the fluid is incompressible, $\boldsymbol{V}$ is a constant vector.

At high velocity the flow can be described by a general form of the non-linear law (e.g., [15]):

$$-(\mathbf{grad}\, P) \cdot \boldsymbol{e}_1 = \frac{\mu}{K_\mathrm{D}} V + F(V). \tag{4}$$

$K_\mathrm{D}$ is the permeability of the Darcy flow; $V$ is the absolute value of the macroscopic velocity vector, $F$ is the non-linear deviation from Darcy's law. For a range of low Reynolds numbers: $Re = \rho V d/\mu$, this deviation is generally assumed to be cubic. When $Re$ grows, this deviation is expected to become quadratic. However, our numerical analysis has revealed another evolution of the macroscopic law.

## 3. Periodic flow

### 3.1. Numerical approach

First of all, we analysed the periodic flow at the macroscale, i.e., the flow velocity distribution was assumed to be identical in the inlet and outlet sections. As the formulated problem has no analytical solution, we solved it numerically, by using the package CFD-ACE based on the finite volume method. The simulation of a periodic flow is possible due to an option of CFD package which enables to define a periodicity of velocity and a modified pressure $p + fx_1$, where $f$ is the absolute value of the volumetric force directed along $x_1$. This modified pressure is introduced in the *body force* option of CFD-GUI [16], using the obvious equivalence: $\mathbf{grad}(p + f \cdot x_1) = \mathbf{grad}\, p - f\boldsymbol{e}_1$. The function $f$ may be selected in such a way that the modified pressure becomes periodic. As shown in [18], $f$ should be equal to the macroscopic pressure gradient over the cell.

We modelled a plane periodic flow for two various sizes of the cell: (i) a cell with a big cavity: $d = 2$, $e = 1$, $L = 4$ and $L' = 2$ (arbitrary units), and (ii) a cell with a small cavity: $d = 2$, $e = 0.5$, $L = 3$ and $L' = 1$. The inlet and the outlet velocities were equal, as were the modified pressures. Function $f$ was a constant parameter, which implies a constant pressure difference along $x_1$. The spatial discretisation method uses a first-order upwind scheme.

### 3.2. Streamlines deformation

In both cases, the observed streamlines reveal two zones in the cell (Fig. 3): a dead zone (I), and a transport zone (II). In the dead zone the fluid moves slowly, decelerated by viscous friction, forming two big vortexes which are

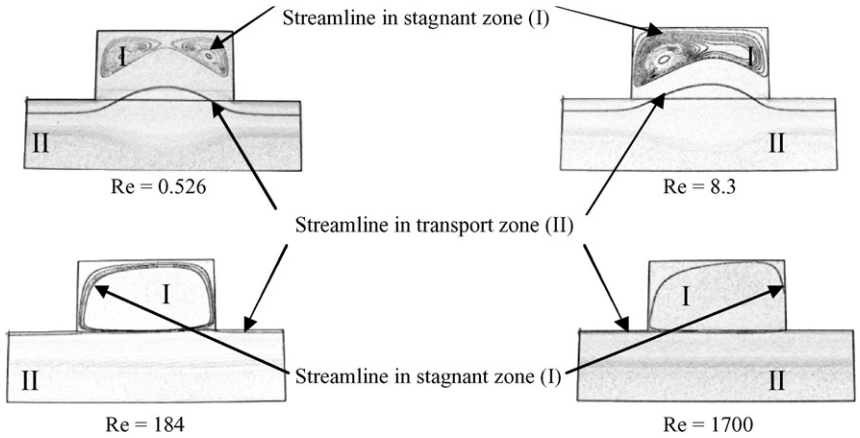


Fig. 3. Streamlines for different Reynolds numbers.

then collapsed into one while the Reynolds number increases. The detailed streamline pattern evolution corresponds well to that described in [3], confirming the validity of our simulation. No mass transfer between both zones was observed, at any $Re$.

In the transport zone the fluid velocity is much higher than in the dead zone. The streamlines are almost straight near the symmetry axis, and slightly curved in front of the cavity. The streamline curvature decreases with the Reynolds number, as observed in [11], due to the microscopic inertial effects. When the Reynolds number is high the streamlines become similar to those in a flow between two horizontal plates, like in a Hele–Shaw cell of thickness $d$. The example of a laminar and stable flow for $Re = 1700$, probably impossible in practice but enabled by CFD-ACE, shows that the streamlines are quite similar to those for $Re = 184$.

This *a priori* qualitative analysis leads us to believe that the macroscopic flow law is likely to vary sharply between $Re = 0$ and $Re = 184$, whereas it will vary much less between $Re = 184$ and $Re = 1700$. This expectation was born out by a quantitative study.

### 3.3. Various non-linear forms of the flow law

In order to analyse the deviation from Darcy's law, let us introduce apparent permeability ($K_{app}$), applying the formal Darcy law instead of (4):

$$\frac{P(0) - P(L)}{L} = \frac{\mu}{K_{app}} V, \tag{5}$$

where $K_{app}$ is obviously a function of velocity. At the same time, let us introduce a constant permeability of the uniform channel which corresponds to the transport zone only: $K_0 = d^2/12$. The following relation between $K_{app}$ and $K_0$ can be obtained from (4) and (5):

$$\frac{K_0}{K_{app}} = \frac{K_0}{K_D} + \frac{K_0}{\mu}\frac{F(V)}{V}. \tag{6}$$

If the deviation from Darcy's law is quadratic, then $F(V) = aV^2$, where $a$ is a constant value [17]. Then the appropriate representation of $K_0/K_{app}$ versus velocity or Reynolds number will be linear:

$$\frac{K_0}{K_{app}} = \frac{K_0}{K_D} + \frac{K_0}{\mu} aV. \tag{7}$$

If the deviation from Darcy's law is cubic, then $F(V) = bV^3$ , where $b$ is a constant value [17]. Then $K_0/K_{app}$ versus $V^2$ or $Re^2$ is linear:

$$\frac{K_0}{K_{app}} = \frac{K_0}{K_D} + \frac{K_0}{\mu} bV^2. \tag{8}$$

These relations were used when processing the simulation results.

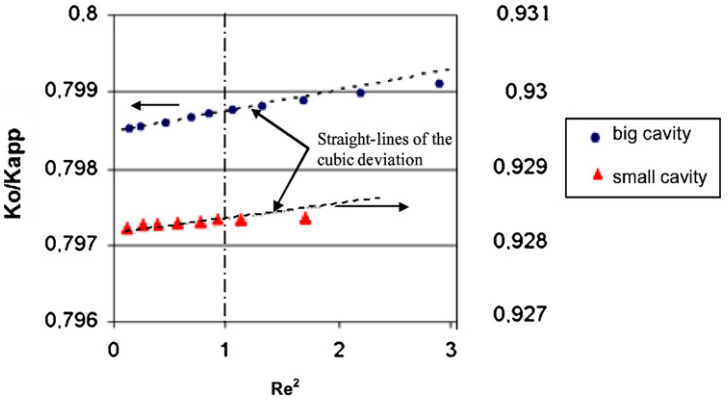


Fig. 4. Cubic deviation for the two cavities.

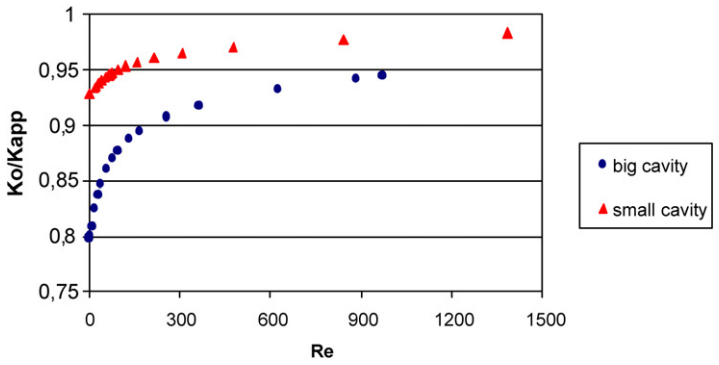


Fig. 5. Permeability ratio versus Reynolds number.

### 3.4. Results of the simulation

The results of our numerical simulations are presented in Figs. 4 and 5. We can observe a variation of $K_0/K_{\text{app}}$ depending on the Reynolds number.

#### 3.4.1. Weak inertia regime

Within the range of low Reynolds numbers, $Re \sim 1$, the cubic deviation was obtained, as shown in Fig. 4. The range of $Re$ for which the cubic deviation remains valid, is larger for a bigger cavity in which the total viscous dissipation is higher. For a higher flow velocity, the viscous dissipation is equilibrated by the inertial force [18].

#### 3.4.2. Strong inertia regime

When the Reynolds number increases, both for the small and the big cavity, the non-linear deviation is non-quadratic, as illustrated in Fig. 5. The permeability ratio tends asymptotically to 1 when $Re$ tends to infinity. As stated previously, in practice the laminar regimes for such a high Reynolds number are impossible, becoming non-stationary and unstable, but they are allowed within an a priori stationary numerical algorithm. Fig. 5 confirms the fact that the macroscopic flow law remains invariable from $Re \sim 200$.

### 3.5. Flow regimes

Relations (7) and (8) can be rewritten using a power-value law for the function $F(V) = \beta V^{\alpha}$

$$\ln\left(\frac{K_0}{K_{\text{app}}} - \frac{K_0}{K_{\text{D}}}\right) = \ln\left(\frac{K_0}{\mu}\right) + \alpha \ln(V) + \ln(\beta). \tag{9}$$

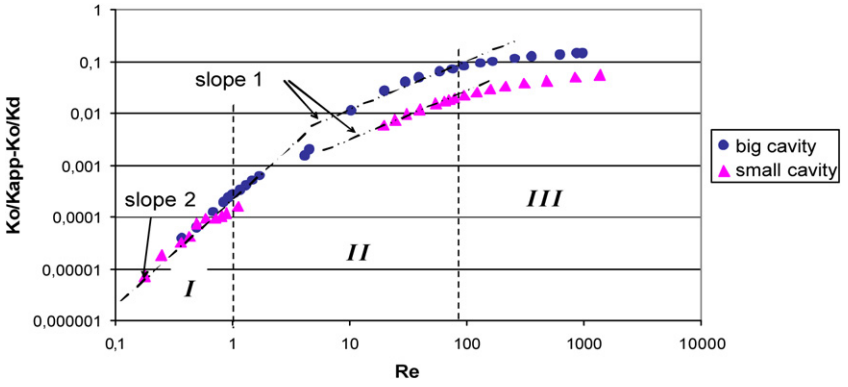


Fig. 6. Modified permeability ratio versus *Re* in logarithmic scale.

Herein $\alpha = 2$ for the cubic flow and $\alpha = 1$ for the quadratic law. For this kind of regime, the function $(K_0/K_{\text{app}} - K_0/K_{\text{D}})$ versus $V$ (or $Re$) is a straight-line of slope $\alpha$ in logarithmic scale. The data obtained numerically are shown in Fig. 6.

The graph shows three characteristic zones:

(i) a cubic zone I: at the beginning, $Re \sim 1$, all the points are superimposed along a straight-line of slope 2; the flow law is cubic ($\alpha = 2$)

$$\ln\left(\frac{K_0}{K_{\text{app}}} - \frac{K_0}{K_{\text{D}}}\right) = \ln\left(\frac{K_0}{\mu}\right) + \ln(\beta) + 2\ln(V). \tag{10}$$

The value of $\beta$ is the same for both cavities. In this regime, the cavity size has no influence on the streamlines pattern, which remains rather regular. All the points are aligned along the same straight-line;

(ii) a "self-similar regime" at very high $Re$ (III): the curves clearly tend to a behaviour independent of $Re$. The left-hand limit of this zone does not seem to depend on the cavity size, which implies that the flow structure is basically imposed by the transport zone, rather than by the cavity. For higher Reynolds numbers, the streamlines are almost horizontal, so the velocity variations tend to zero, the inertial effects decrease and $\alpha$ becomes lower than 1;

(iii) a transition zone II: the points vary monotonically between the cubic zone and the self-similar regime. For a smaller cavity the transition regime appears at lower $Re$. The non-linear term varies progressively from the cubic one to zero [19], even though several points are almost aligned on a straight-line of slope 1, no clear quadratic behaviour is observed.

Thus, the simulation for a periodic flow confirms the existence of a cubic deviation, a self-similar regime independent of $Re$, and does not confirm the existence of the strictly quadratic law. This is in agreement with the analysis presented in the Introduction, when we noted that in a symmetric (periodic) flow the even powers of velocity should disappear.

## 4. Non-periodic flow

For the next step, we analysed the non-periodic flow structure, the objective being to reveal the role of the flow asymmetry on the form on the non-linear correction.

### *4.1. Model*

The non-periodic flow was analysed for a unique cavity, as the qualitative results do not depend on the cavity size: $d = 2$, $e = 1$, $L = 4$ and $L' = 2$ (see Fig. 1).

To model a natural non-periodic flow, we examined a set of consecutive cells, imposing a uniform velocity profile, $\boldsymbol{U}$, at the inlet and the outlet boundaries. At the same time, only the central cell was treated in terms of the macroscopic

Table 1
Quantitative characteristics of qualitative non-periodicity degrees

| Geometric establishment length (in length of pattern/$d$) | Number of cells ($2n+1$) | Non-periodicity degree |
|---|---|---|
| 2.5 | 13 | almost periodic |
| 2.5 | 7 | non-periodic+ |
| 2.5 | 1 | non-periodic++ |
| 0.125 | 1 | highly non-periodic+++ |

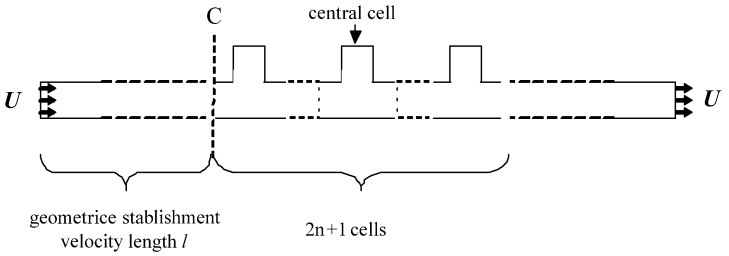


Fig. 7. The non-periodic flow model.

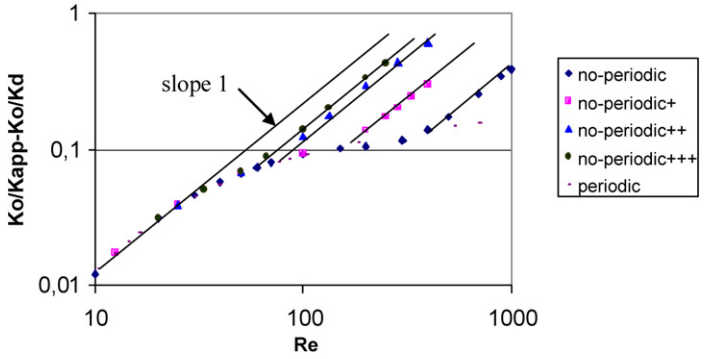


Fig. 8. Quadratic deviation in a non-periodic flow.

flow law. Between the inlet section and section C (Fig. 7), corresponding to a so-called geometric establishment length, the velocity profiles progressively vary from a uniform profile to the Poiseuille parabolic profile in section C. The flow profile in this cell is closer to the periodic one when the number of cells increases and/or the establishment length also increases. A qualitative geometric scale of non-periodicity, independent of the Reynolds number, can therefore be defined based on these characteristics which are considered as two origins of non-periodicity,.

By increasing the number of cells and reducing $l$, we reduce the flow non-periodicity degree. In Table 1 several non-periodic cases with a different non-periodicity degree are presented, from an "almost periodic" to a "high non-periodic" (+++).

### 4.2. Results

Several simulations were performed by varying the number of cells and the establishment length. These simulations showed, in Fig. 8, that a strictly quadratic deviation can appear in the case of a non-periodic porous medium, where the slope $\alpha$ of the solid lines is strictly equal to 1. The higher the non-periodicity degree, the lower the Reynolds number marking the beginning of deviations from Darcy's law, as shown in Fig. 8. Furthermore, as the intercept, in logarithmic scale, of the straight-lines is higher when $Re$ grows, it means that the quadratic effects are all the more important as $Re$ is high.

Contrary to the periodic case of flow, the value $K_0/K_{\text{app}}$ varies without stabilising when the Reynolds number tends to infinity. The comparison between the periodic and non-periodic case shows that two effects are in competition.

Indeed, the periodic behaviour is also partially observed in the non-periodic case, all the more as the flow is less non-periodic. A straightening of the streamlines by the inertia forces reduces the non-linear effects. But non-periodicity changes the flow structure, only microscopically. Indeed the streamlines in the central cell are similar to those of the periodic case. No macroscopic difference can be observed, the flow structure is still imposed by the thin channel. The effect of the inertial forces makes the deviation quadratic. This qualitative change has important quantitative consequences, which have to be evaluated from the microscopic flow structure.

## 5. Estimation of the quadratic deviation

The non-linear deviation is determined by the macroscopic inertia effect which can be evaluated by integrating the microscopic inertial term $v_i \partial \boldsymbol{v}/\partial x_i$ over the cell. At high Reynolds numbers, when the inertia forces straighten the streamlines, the following may be accepted:

(i) all the streamlines in the inlet and the outlet section are straight, as shown in Fig. 9:

$$v_2 \approx 0 \quad \text{and} \quad \frac{\partial v_2}{\partial x_1} \approx 0; \tag{11}$$

(ii) the velocity field in the dead zone is negligible compared to that in the transport zone.

The homogenisation over the cell of the inertial term projection on axe $x_1$, $v_i \partial \boldsymbol{v}_1/\partial x_i$, yields:

$$\left\langle v_i \frac{\partial \boldsymbol{v}_1}{\partial x_i} \right\rangle \approx \left\langle v_1 \frac{\partial \boldsymbol{v}_1}{\partial x_1} \right\rangle_{\text{tr}} \cdot \boldsymbol{e}_1 = \frac{\boldsymbol{e}_1}{2} \int_0^{d/2} \left( v_1^2(L, x_2) - v_1^2(0, x_2) \right) \mathrm{d}x_2, \tag{12}$$

where the symbol $\langle \cdot \rangle$ means the integration over the entire cell, while $\langle \cdot \rangle_{\text{tr}}$ is the integration over the transport zone only.

For a non-periodic flow configuration, we can express the microscopic velocity through the macroscopic velocity: $v_1(L, x_2) = \lambda_1(x_2) V$ and $v_1(0, x_2) = \lambda_1(x_2) V$, where $\lambda_1(x_2)$ and $\lambda_2(x_2)$ are empirical functions. Thus, it follows:

$$\left\langle v_i \frac{\partial \boldsymbol{v}_1}{\partial x_i} \right\rangle \approx b V^2 \boldsymbol{e}_1 \quad \text{with } b = \frac{1}{2} \int_0^{d/2} \left( \lambda_1^2(x_2) - \lambda_2^2(x_2) \right) \mathrm{d}x_2. \tag{13}$$

Thus, the inertial effect is approximately proportional to the square of the averaged velocity, if $b$ does not depend on the Reynolds number. The simulations show that this parameter $b$ is really independent of the Reynolds number

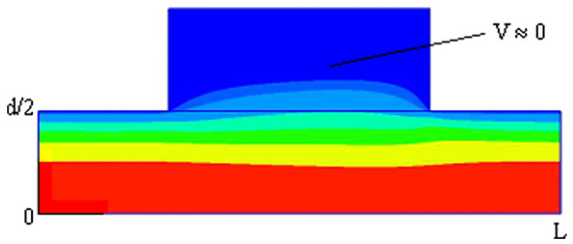


Fig. 9. Velocity distribution in a cell.

Table 2
Values of parameter $b$ for various non-periodicity degrees, at a fixed $Re$

| | $b$ |
|---|---|
| almost periodic | 0.00115 |
| non-periodic+ | 0.00255 |
| non-periodic++ | 0.00490 |
| highly non-periodic+++ | 0.00580 |

and remains constant for a given medium shape (Table 2). Moreover, the simulations show an increase of $b$ when the non-periodicity degree increases, which is in agreement with the numerical analysis presented in Section 4.

We also notice that the previous demonstration, with its adopted simplifications, can explain that, for a periodic flow, the macroscopic inertial effects tend to zero when the Reynolds number tends to infinity: indeed, in this case $\lambda_1 = \lambda_2$, and consequently $b = 0$.

## 6. Conclusions

In the case of periodic flow several ranges of the Reynolds number have been identified for which the deviation from Darcy's law progressively varies from a cubic zone, through a transition non-quadratic zone to a "self-similar" mode. In the self-similar regime, the inertia effect decreases when *Re* grows, due to straightening the streamlines. This confirms theoretical results for periodic flow which prohibit the even velocity powers in the macroscopic law.

Non-periodicity is shown to be a major factor which may determine the appearance of a quadratic term. The quadratic deviation appears at lower Re if the non-periodicity degree increases.

The previous remark may provide an explanation of the fact that so many experiments and numerical simulations have seemed to prove that the quadratic term appeared in the periodic case. Indeed, it is experimentally almost impossible and sometimes numerically very difficult to achieve a perfect periodic flow [20,21]. Thus, which is supposed to be a quadratic deviation in a periodic flow would be actually caused by non-periodicity. As said in introduction, one way to solve contradictions linked to the quadratic law between some theoretical remarks and some observations is to take flow asymmetry into account.

## References

[1] M. Rasoloarijaona, J.-L. Auriault, Non-linear seepage flow through a rigid porous medium, European Journal of Mechanics B/Fluids 13 (2) (1994) 177–195.
[2] G. Chauvetau, C. Thirriot, Régimes d'écoulement en milieu poreux et limite de la loi de Darcy, La Houille Blanche 2 (1967) 141–148.
[3] D. Ruth, H. Ma, On the derivation of the Forchheimer equation by means of the averaging theorem, Transport in Porous Media 7 (1992) 255–264.
[4] A. Levy, D. Levi-Hevroni, S. Sorek, G. Ben-Dor, Derivation of Forchheimer terms and their verification by application to waves propagation in porous media, International Journal of Multiphase Flow 25 (1999) 683–704.
[5] I. Panfilova, M. Buès, M. Panfilov, Hig-hrate Navier–Stokes flow in porous media: d'Alembert paradox and its solution, in: Auriault, et al. (Eds.), Poromechanics II, Second Biot Conference on Poromechanics, Grenoble, France, August 26–28, 2002, Swets & Zeitlinger, Lisse, ISBN 90-5809-394-8, 2000, pp. 495–500.
[6] M. Panfilov, C. Oltean, I. Panfilova, M. Buès, Singular nature of non-linear macroscale effects in high-rate flow through porous media, C. R. Mecanique 331 (2003) 41–48.
[7] M. Firdaous, J.-L. Guermond, Sur l'homogénéisation des équations de Navier–Stokes à faible nombre de Reynolds, C. R. Acad. Sci. Paris, Sér. I 320 (1995) 245–251.
[8] T. Levy, Loi de Darcy ou loi de Brinkman?, C. R. Acad. Sci. Paris, Sér. II 292 (1981) 871–874.
[9] J.-C. Wodie, T. Levy, Correction non linéaire de la loi de Darcy, C. R. Acad. Sci. Paris, Sér. II 312 (1991) 157–161.
[10] J.-C. Wodie, Contribution à l'étude des milieux poreux par la méthode de l'homogénéisation : filtration non linéaire, milieux fissurés, Thèse de l'Université de Paris VI, 1992, 212 pp.
[11] E. Skjetne, J.-L. Auriault, High-velocity laminar and turbulent flow in porous media, Transport in Porous Media 36 (1999) 131–147.
[12] F. Lusseyran, P. Gougat, Y. Fraigneau, A.E. Gafsi, Caractéristiques spatiales et temporelles de modes instables en cavité ouverte, in : XVI$^{\text{ème}}$ Congrès Français de Mécanique, 1–5 septembre 2003. CD Cfm2003.
[13] M. Buès, M. Panfilov, S. Crosnier, C. Oltéan, Macroscale model and viscous inertia effect, for Navier–Stokes flow in a radial fracture with corrugated walls, Journal of Fluid Mechanics 504 (2004) 41–60.
[14] S. Sisavath, A. Al-Yaarubi, C. Pain, R.W. Zimmerman, A simple model for deviation from the cubic law for a fracture undergoing dilation or closure, Pure and Applied Geophysics 160 (2003) 1009–1022.
[15] S. Crosnier, S. Chevalier, M. Buès, Comparison between numerical simulations and experimental investigations of radial flows in rough fracture, in: M. Ralmand, C.A. Brebbia (Eds.), Advances in Fluid Mechanics III, WIT Press, ISBN 1-85312-813-9, 2000, pp. 43–52.
[16] CFD-ACE, CFDRC, On the leading edge of CFD technology, 9 volumes, version 5, 1998.
[17] R.W. Zimmerman, A. Al-Yaarubi, C.C. Pain, C.A. Grattoni, Non-linear regimes of flow in rock fractures, Int. J. Rock Mech. (Supp. 1) 41 (2004) 163–169.
[18] M. Panfilov, M. Fourar, Physical splitting of non-linear effects in high-velocity stable flow through porous media, Advances in Water Resources 29 (1) (2005) 30–41.
[19] C.C. Mei, J.-L. Auriault, The effect of weak inertia on flow through a porous medium, Journal of Fluid Mechanics 222 (1990) 647–663.
[20] D. Koch, A. Ladd, Moderate Reynolds number flows through periodic and random arrays of aligned cylinders, Journal of Fluid Mechanics 349 (1997) 31–66.
[21] A. Bourgeat, E. Marusic-Paloka, Loi d'écoulement non linéaire entre deux plaques ondulées, C. R. Acad. Sci. Paris, Sér. I 321 (1995) 1115–1120.